

Impact of Forward-Backward Asymmetry on SMEFT fits with high m_{ll} Drell-Yan data

Yingsheng Huang

Northwestern U. & Argonne

In collaboration with:

Radja Boughezal and Frank Petriello



Northwestern
University

arxiv: 2304.11142

June 26th @ LoopFest XXI



1 Introduction

2 AFB in NC Drell-Yan

3 Results

- Linear contributions only
- Quadratic contributions

4 Summary

- ◇ No conclusive evidence of new physics, suggest new physics is probably above TeV scale
- ◇ Limitations of current experiments motivate indirect searches that probe deviations from SM predictions

- ◇ No conclusive evidence of new physics, suggest new physics is probably above TeV scale
- ◇ Limitations of current experiments motivate indirect searches that probe deviations from SM predictions
- Standard Model Effective Field Theory (SMEFT)
 - extension to SM
 - degrees of freedom & symmetries of SM
 - power counting: new physics scale Λ

$$\mathcal{L}_{\text{SMEFT}} = \mathcal{L}_{\text{SM}} + \frac{1}{\Lambda^2} \sum C_6 \mathcal{O}_6 + \frac{1}{\Lambda^4} \sum C_8 \mathcal{O}_8 + \dots$$

- ▶ omitting odd dimensions due to lepton & baryon number violation
- ▶ \mathcal{L}_6 (Warsaw basis): 76 B-preserving Lagrangian terms, 2499 parameters
Grzadkowski et al. 2010
- ▶ \mathcal{L}_8 : 1031 Lagrangian terms, 44807 parameters [Murphy 2020](#); [Li et al. 2021](#)
- ▶ Non-redundant basis known up to dimension-12: [2305.06832](#)

X^3		φ^6 and $\varphi^4 D^2$		$\psi^2 \varphi^3$	
Q_G	$f^{ABC} G_{\mu\nu}^A G_{\nu\rho}^B G_{\rho\mu}^C$	$Q_{\varphi\varphi}$	$(\varphi^\dagger \varphi)^3$	$Q_{e\varphi}$	$(\varphi^\dagger \varphi)(\bar{l}_p e_r \varphi)$
$Q_{\bar{G}}$	$f^{ABC} \bar{G}_{\mu\nu}^A G_{\nu\rho}^B G_{\rho\mu}^C$	$Q_{\varphi\Box}$	$(\varphi^\dagger \varphi)\Box(\varphi^\dagger \varphi)$	$Q_{u\varphi}$	$(\varphi^\dagger \varphi)(\bar{q}_p u_r \varphi)$
Q_W	$\varepsilon^{IJK} W_{\mu\nu}^I W_{\nu\rho}^J W_{\rho\mu}^K$	$Q_{\varphi D}$	$(\varphi^\dagger D^\mu \varphi)^* (\varphi^\dagger D_\mu \varphi)$	$Q_{d\varphi}$	$(\varphi^\dagger \varphi)(\bar{q}_p d_r \varphi)$
$Q_{\bar{W}}$	$\varepsilon^{IJK} \bar{W}_{\mu\nu}^I W_{\nu\rho}^J W_{\rho\mu}^K$				

$X^2 \varphi^2$		$\psi^2 X \varphi$		$\psi^2 \varphi^2 D$	
$Q_{\varphi G}$	$\varphi^\dagger \varphi G_{\mu\nu}^A G^{A\mu\nu}$	Q_{eW}	$(\bar{l}_p \sigma^{\mu\nu} e_r) \tau^I \varphi W_{\mu\nu}^I$	$Q_{\varphi l}^{(1)}$	$(\varphi^\dagger i D_\mu \varphi)(\bar{l}_p \gamma^\mu l_r)$
$Q_{\varphi \bar{G}}$	$\varphi^\dagger \varphi \bar{G}_{\mu\nu}^A G^{A\mu\nu}$	Q_{eB}	$(\bar{l}_p \sigma^{\mu\nu} e_r) \varphi B_{\mu\nu}$	$Q_{\varphi l}^{(2)}$	$(\varphi^\dagger i D_\mu^\dagger \varphi)(\bar{l}_p \tau^I \gamma^\mu l_r)$
$Q_{\varphi W}$	$\varphi^\dagger \varphi W_{\mu\nu}^I W^{I\mu\nu}$	Q_{uG}	$(\bar{q}_p \sigma^{\mu\nu} u_r) \tau^A \varphi G_{\mu\nu}^A$	$Q_{\varphi e}$	$(\varphi^\dagger i D_\mu \varphi)(\bar{e}_p \gamma^\mu e_r)$
$Q_{\varphi \bar{W}}$	$\varphi^\dagger \varphi \bar{W}_{\mu\nu}^I W^{I\mu\nu}$	Q_{uW}	$(\bar{q}_p \sigma^{\mu\nu} u_r) \tau^I \varphi W_{\mu\nu}^I$	$Q_{\varphi q}^{(1)}$	$(\varphi^\dagger i D_\mu \varphi)(\bar{q}_p \gamma^\mu q_r)$
$Q_{\varphi B}$	$\varphi^\dagger \varphi B_{\mu\nu} B^{\mu\nu}$	Q_{uB}	$(\bar{q}_p \sigma^{\mu\nu} u_r) \varphi B_{\mu\nu}$	$Q_{\varphi q}^{(2)}$	$(\varphi^\dagger i D_\mu^\dagger \varphi)(\bar{q}_p \tau^I \gamma^\mu q_r)$
$Q_{\varphi \bar{B}}$	$\varphi^\dagger \varphi \bar{B}_{\mu\nu} B^{\mu\nu}$	Q_{dG}	$(\bar{q}_p \sigma^{\mu\nu} T^A d_r) \varphi G_{\mu\nu}^A$	$Q_{\varphi u}$	$(\varphi^\dagger i D_\mu \varphi)(\bar{u}_p \gamma^\mu u_r)$
$Q_{\varphi WB}$	$\varphi^\dagger \tau^I \varphi W_{\mu\nu}^I B^{\mu\nu}$	Q_{dW}	$(\bar{q}_p \sigma^{\mu\nu} d_r) \tau^I \varphi W_{\mu\nu}^I$	$Q_{\varphi d}$	$(\varphi^\dagger i D_\mu \varphi)(\bar{d}_p \gamma^\mu d_r)$
$Q_{\varphi \bar{W}B}$	$\varphi^\dagger \tau^I \varphi \bar{W}_{\mu\nu}^I B^{\mu\nu}$	Q_{dB}	$(\bar{q}_p \sigma^{\mu\nu} d_r) \varphi B_{\mu\nu}$	$Q_{\varphi ud}$	$i(\bar{\varphi}^\dagger D_\mu \varphi)(\bar{u}_p \gamma^\mu d_r)$

$(\bar{L}L)(\bar{L}L)$		$(\bar{R}R)(\bar{R}R)$		$(\bar{L}L)(\bar{R}R)$	
Q_{ll}	$(\bar{l}_p \gamma_\mu l_r)(\bar{l}_s \gamma^\mu l_t)$	Q_{ee}	$(\bar{e}_p \gamma_\mu e_r)(\bar{e}_s \gamma^\mu e_t)$	Q_{le}	$(\bar{l}_p \gamma_\mu l_r)(\bar{e}_s \gamma^\mu e_t)$
$Q_{qq}^{(1)}$	$(\bar{q}_p \gamma_\mu q_r)(\bar{q}_s \gamma^\mu q_t)$	Q_{uu}	$(\bar{u}_p \gamma_\mu u_r)(\bar{u}_s \gamma^\mu u_t)$	Q_{lu}	$(\bar{l}_p \gamma_\mu l_r)(\bar{u}_s \gamma^\mu u_t)$
$Q_{qq}^{(3)}$	$(\bar{q}_p \gamma_\mu \tau^I q_r)(\bar{q}_s \gamma^\mu \tau^I q_t)$	Q_{dd}	$(\bar{d}_p \gamma_\mu d_r)(\bar{d}_s \gamma^\mu d_t)$	Q_{ld}	$(\bar{l}_p \gamma_\mu l_r)(\bar{d}_s \gamma^\mu d_t)$
$Q_{ll}^{(1)}$	$(\bar{l}_p \gamma_\mu l_r)(\bar{q}_s \gamma^\mu q_t)$	Q_{eu}	$(\bar{e}_p \gamma_\mu e_r)(\bar{u}_s \gamma^\mu u_t)$	Q_{qe}	$(\bar{q}_p \gamma_\mu q_r)(\bar{e}_s \gamma^\mu e_t)$
$Q_{ll}^{(3)}$	$(\bar{l}_p \gamma_\mu \tau^I l_r)(\bar{q}_s \gamma^\mu \tau^I q_t)$	Q_{ed}	$(\bar{e}_p \gamma_\mu e_r)(\bar{d}_s \gamma^\mu d_t)$	$Q_{qu}^{(1)}$	$(\bar{q}_p \gamma_\mu q_r)(\bar{u}_s \gamma^\mu u_t)$
		$Q_{ud}^{(1)}$	$(\bar{u}_p \gamma_\mu u_r)(\bar{d}_s \gamma^\mu d_t)$	$Q_{qu}^{(8)}$	$(\bar{q}_p \gamma_\mu T^A q_r)(\bar{u}_s \gamma^\mu T^A u_t)$
		$Q_{ud}^{(8)}$	$(\bar{u}_p \gamma_\mu T^A u_r)(\bar{d}_s \gamma^\mu T^A d_t)$	$Q_{qd}^{(1)}$	$(\bar{q}_p \gamma_\mu q_r)(\bar{d}_s \gamma^\mu d_t)$
				$Q_{qd}^{(8)}$	$(\bar{q}_p \gamma_\mu T^A q_r)(\bar{d}_s \gamma^\mu T^A d_t)$

$(\bar{L}R)(\bar{R}L)$ and $(\bar{L}R)(\bar{L}R)$		B-violating	
Q_{ledq}	$(\bar{l}_p^j e_r)(\bar{d}_s^k q_t^j)$	Q_{duq}	$\varepsilon^{\alpha\beta\gamma} \varepsilon_{jk} [(d_p^\alpha)^T C u_r^\beta] [(q_s^\gamma)^T C q_t^k]$
$Q_{quqd}^{(1)}$	$(\bar{q}_p^j u_r) \varepsilon_{jk} (\bar{q}_s^k d_t)$	Q_{quq}	$\varepsilon^{\alpha\beta\gamma} \varepsilon_{jk} [(q_p^\alpha)^T C q_r^\beta] [(u_s^\gamma)^T C e_t]$
$Q_{quqd}^{(8)}$	$(\bar{q}_p^j T^A u_r) \varepsilon_{jk} (\bar{q}_s^k T^A d_t)$	Q_{quq}	$\varepsilon^{\alpha\beta\gamma} \varepsilon_{jkm} [(q_p^\alpha)^T C q_r^\beta] [(q_s^\gamma)^T C q_t^m]$
$Q_{lequ}^{(1)}$	$(\bar{l}_p^j e_r) \varepsilon_{jk} (\bar{q}_s^k u_t)$	Q_{duu}	$\varepsilon^{\alpha\beta\gamma} [(d_p^\alpha)^T C u_r^\beta] [(u_s^\gamma)^T C e_t]$
$Q_{lequ}^{(3)}$	$(\bar{l}_p^j \sigma_{\mu\nu} e_r) \varepsilon_{jk} (\bar{q}_s^k \sigma^{\mu\nu} u_t)$		

- Relevant to Drell-Yan at tree-level

- Minimal flavor violation (MFV):

Yukawa terms are the only sources of flavor symmetry violation

- 3 relevant categories:

- $\psi^2 X \varphi$
- $\psi^2 \varphi^2 D$
- ψ^4

- Study scaling of cross sections in high energy limit (Mandelstam s , Higgs vev. v)
- Only show some examples for each category
- q, l : left-handed fermion doublets
 e, u, d : right-handed fermion singlets
 ϕ : Higgs doublet

$$\mathcal{L}_{\psi^2 X \phi}$$

$$\frac{C_{eB}}{\Lambda^2} \bar{l} \sigma^{\mu\nu} B_{\mu\nu} \phi e$$

$$\frac{C_{uW}}{\Lambda^2} \bar{q} \sigma^{\mu\nu} \tau^I W_{\mu\nu}^I \phi u$$

Dipole coupling

assume massless fermion

$$\sim \mathcal{O}(v^2 s / \Lambda^4)$$

$$\mathcal{L}_{\psi^2 \phi^2 D}$$

$$\frac{C_{Hl}^{(1)}}{\Lambda^2} \phi^\dagger \overleftrightarrow{D}^\mu \phi \bar{l} \gamma_\mu l$$

$$\frac{C_{Hu}}{\Lambda^2} \phi^\dagger \overleftrightarrow{D}^\mu \phi \bar{u} \gamma_\mu u$$

Z-vertex corrections

$$\sim \mathcal{O}(v^2 / \Lambda^2)$$

$$\mathcal{L}_{\psi^4}$$

$$\frac{C_{lq}^{(1)}}{\Lambda^2} \bar{l} \gamma^\mu l q \gamma_\mu q$$

$$\frac{C_{ld}}{\Lambda^2} \bar{l} \gamma^\mu l d \gamma_\mu d$$

Four-fermion interactions

$$\sim \mathcal{O}(s / \Lambda^2)$$

Dipole coupling & vertex corrections are numerically verified to be much smaller than four fermion operators

- Study scaling of cross sections in high energy limit (Mandelstam s , Higgs vev. v)
- Only show some examples for each category
- q, l : left-handed fermion doublets
- e, τ : right-handed fermion singlets
- ϕ : Higgs

7 dim-6 four-fermion operators (for high m_U data):

$\mathcal{O}_{lq}^{(1)}$	$(\bar{l}\gamma^\mu l)(\bar{q}\gamma_\mu q)$	\mathcal{O}_{lu}	$(\bar{l}\gamma^\mu l)(\bar{u}\gamma_\mu u)$
$\mathcal{O}_{lq}^{(3)}$	$(\bar{l}\gamma^\mu \tau^I l)(\bar{q}\gamma_\mu \tau^I q)$	\mathcal{O}_{ld}	$(\bar{l}\gamma^\mu l)(\bar{d}\gamma_\mu d)$
\mathcal{O}_{eu}	$(\bar{e}\gamma^\mu e)(\bar{u}\gamma_\mu u)$	\mathcal{O}_{qe}	$(\bar{q}\gamma^\mu q)(\bar{e}\gamma_\mu e)$
\mathcal{O}_{ed}	$(\bar{e}\gamma^\mu e)(\bar{d}\gamma_\mu d)$		

Dipole coupling

Z-vertex corrections

Four-fermion interactions

assume massless fermion

$$\sim \mathcal{O}(v^2 s / \Lambda^4)$$

$$\sim \mathcal{O}(v^2 / \Lambda^2)$$

$$\sim \mathcal{O}(s / \Lambda^2)$$

Dipole coupling & vertex corrections are numerically verified to be much smaller than four fermion operators

Flat directions

degeneracies among Wilson coefficients

Example:

Total cross section $\sigma \propto C_1 + C_2$



σ can not distinguish Wilson coefficients C_1 and C_2

Flat directions

degeneracies among Wilson coefficients

Four fermion operators in Drell-Yan:

- Flat directions in low-energy observables

[Falkowski, González-Alonso, and Mimouni 2017](#)

- and high m_U bins at hadron colliders

[Alte, König, and Shepherd 2019](#)

Flat directions

degeneracies among Wilson coefficients

Four fermion operators in Drell-Yan:

- Flat directions in low-energy observables

[Falkowski, González-Alonso, and Mimouni 2017](#)

- and high m_U bins at hadron colliders

[Alte, König, and Shepherd 2019](#)

One solution: future experiments that probe independent combinations of coefficients

Flat directions

degeneracies among Wilson coefficients

Four fermion operators in Drell-Yan:

- Flat directions in low-energy observables

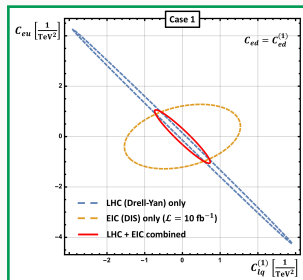
Falkowski, González-Alonso, and Mimouni 2017

- and high m_U bins at hadron colliders

Alte, König, and Shepherd 2019

One solution: future experiments that probe independent combinations of coefficients

- EIC Boughezal, Petriello, and Wiegand 2020



Flat directions

degeneracies among Wilson coefficients

Four fermion operators in Drell-Yan:

- Flat directions in low-energy observables

Falkowski, González-Alonso, and Mimouni 2017

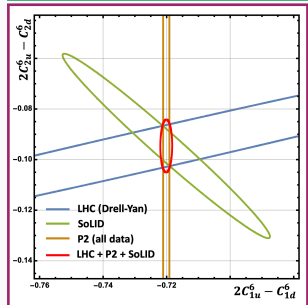
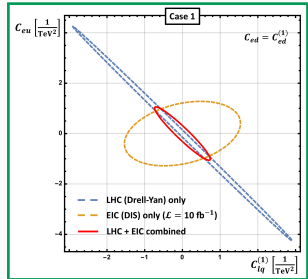
- and high m_U bins at hadron colliders

Alte, König, and Shepherd 2019

One solution: future experiments that probe independent combinations of coefficients

- EIC Boughezal, Petriello, and Wiegand 2020
- low energy Parity-Violating Electron Scattering (PVES)

Boughezal, Petriello, and Wiegand 2021



Flat directions

degeneracies among Wilson coefficients

Four fe

- Flat
- Fall
- an
- Alt

One so

dependent combinations of coefficients

- EIC Boughezal, Petriello, and Wiegand 2020
- low energy Parity-Violating Electron Scattering (PVES)

Boughezal, Petriello, and Wiegand 2021

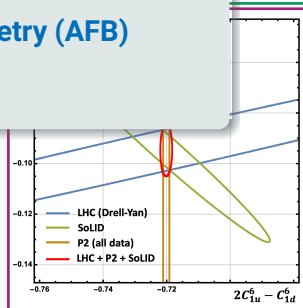
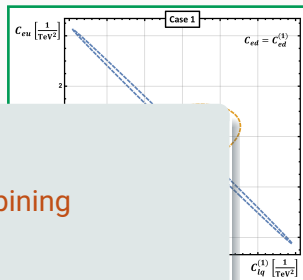
This talk:

remove flat directions by combining

– invariant mass dist.

– forward-backward asymmetry (AFB)

at the LHC.



LO SMEFT contributions to partonic cross section in **high energy limit**

$$\frac{d\sigma^x}{dm_{ll}^2 dY dc_\theta} \sim \frac{1}{\Lambda^2} \frac{A_1^x \hat{u}^2 + A_2^x \hat{t}^2}{\hat{s}^2}$$

where $\hat{t} = -\frac{\hat{s}}{2}(1 - c_\theta)$, $\hat{u} = -\frac{\hat{s}}{2}(1 + c_\theta)$, $c_\theta \equiv \cos(\theta)$ (θ : polar angle in parton C.M. frame).

- A_i^x : linear in $C_i^{(6)}$;
- A does not depend on kinematic variables
- x : partonic channel u or d

LO SMEFT contributions to partonic cross section in **high energy limit**

$$\frac{d\sigma^x}{dm_{\hat{t}\hat{t}}^2 dY dc_\theta} \sim \frac{1}{\Lambda^2} \frac{A_1^x \hat{u}^2 + A_2^x \hat{t}^2}{\hat{s}^2}$$

where $\hat{t} = -\frac{\hat{s}}{2}(1 - c_\theta)$, $\hat{u} = -\frac{\hat{s}}{2}(1 + c_\theta)$, $c_\theta \equiv \cos(\theta)$ (θ : polar angle in parton C.M. frame).

condition of a flat direction

u & d channels: same condition of $C_i^{(6)}$ for the SMEFT corrections to vanish

Examples of Wilson coefficients combination (C_1 & C_2)

$$\left\{ \begin{array}{l} \sigma^u \sim C_1 + C_2 \\ \sigma^d \sim C_1 + C_2 \end{array} \right. \Rightarrow \text{same combination in both channels} \Rightarrow \text{flat direction}$$

$$\left\{ \begin{array}{l} \sigma^u \sim C_1 + C_2 \\ \sigma^d \sim C_1 - C_2 \end{array} \right. \Rightarrow \text{different combination in both channels} \Rightarrow \text{no flat direction}$$

LO SMEFT contributions to partonic cross section in **high energy limit**

$$\frac{d\sigma^x}{dm_{ll}^2 dY dc_\theta} \sim \frac{1}{\Lambda^2} \frac{A_1^x \hat{u}^2 + A_2^x \hat{t}^2}{\hat{s}^2}$$

where $\hat{t} = -\frac{\hat{s}}{2}(1 - c_\theta)$, $\hat{u} = -\frac{\hat{s}}{2}(1 + c_\theta)$, $c_\theta \equiv \cos(\theta)$ (θ : polar angle in parton C.M. frame).

Replace \hat{u} , \hat{t} with c_θ

$$\frac{d\sigma^x}{dm_{ll}^2 dY dc_\theta} \sim \frac{1}{4\Lambda^2} [(A_1^x + A_2^x)(1 + c_\theta^2) + 2(A_1^x - A_2^x)c_\theta]$$

- $d\sigma/dm$ is only sensitive to $A_1 + A_2$
- $A_1 - A_2$: vanish under integration over c_θ , can be probed by angular dist.

LO SMEFT contributions to partonic cross section in **high energy limit**

$$\frac{d\sigma^x}{dm_{ll}^2 dY dc_\theta} \sim \frac{1}{\Lambda^2} \frac{A_1^x \hat{u}^2 + A_2^x \hat{t}^2}{\hat{s}^2}$$

where $\hat{t} = -\frac{\hat{s}}{2}(1 - c_\theta)$, $\hat{u} = -\frac{\hat{s}}{2}(1 + c_\theta)$, $c_\theta \equiv \cos(\theta)$ (θ : polar angle in parton C.M. frame).

If C_1 and C_2 exist in A_1 and A_2 separately, angular observables that probe $A_1 - A_2$ may cancel out the flat directions from $A_1 + A_2$

➡ **AFB**

$$\frac{d\sigma^x}{dm_{ll}^2 dY dc_\theta} = \frac{4\Lambda^2}{\hat{s}^2} \left[C_1 \frac{A_1^x \hat{u}^2 + A_2^x \hat{t}^2}{\hat{s}^2} + C_2 \frac{A_1^x \hat{u} - A_2^x \hat{t}}{\hat{s}} \right]$$

- $d\sigma/dm$ is only sensitive to $A_1 + A_2$
- $A_1 - A_2$: vanish under integration over c_θ , can be probed by angular dist.

Forward-backward Asymmetry (AFB)

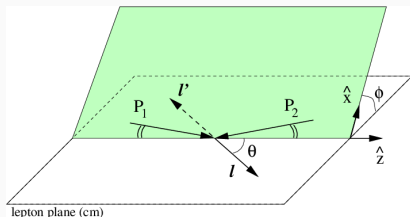
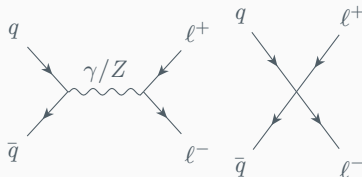
$$A_{\text{FB}} = \frac{\sigma_F - \sigma_B}{\sigma_F + \sigma_B}$$

- depends on Collins-Soper angle θ^*
 - σ_F : forward ($\cos \theta^* > 0$)
 - σ_B : backward ($\cos \theta^* < 0$)

Collins-Soper angle **Collins and Soper 1977**

$$\cos \theta^* = \frac{2(P_1^+ P_2^- - P_1^- P_2^+)}{\sqrt{Q^2(Q^2 + Q_T^2)}} \quad (\text{hadron C.M.})$$

- angle between the incoming quark and the outgoing lepton (negatively charged) in the dilepton rest frame



Forward-backward Asymmetry (AFB)

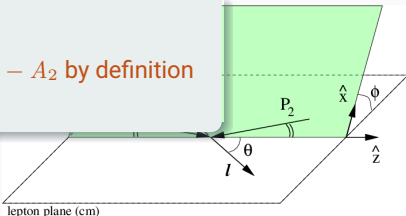
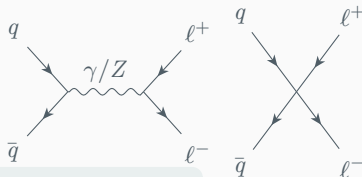
$$A_{\text{FB}} = \frac{\sigma_F - \sigma_B}{\sigma_F + \sigma_B}$$

- depends on Collins-Soper angle θ^*
 - σ_F : forward
 - σ_B : backward

AFB is only sensitive to $A_1 - A_2$ by definition

Collins-Soper angle

$$\cos \theta^* = \frac{2(P_1^+ P_2^- - P_1^- P_2^+)}{\sqrt{Q^2(Q^2 + Q_T^2)}} \quad (\text{hadron C.M.})$$



- angle between the incoming quark and the outgoing lepton (negatively charged) in the dilepton rest frame

SMEFT CORRECTIONS TO CROSS SECTION & AFB

Structure of the SMEFT cross section

$$d\sigma = d\sigma_{\text{SM}} + \sum_i \frac{a_i^{(6)}}{\Lambda^2} C_i^{(6)} + \sum_{i,j} \frac{b_{ij}^{(6)}}{\Lambda^4} C_i^{(6)} C_j^{(6)}$$

Structure of the SMEFT AFB

$$A_{\text{FB}} = A_{\text{FB}}^{\text{SM}} + \sum_i \frac{C_i^{(6)}}{\Lambda^2} \frac{\sigma_{\text{SM}} \Delta a_i^{(6)} - a_i^{(6)} \Delta \sigma_{\text{SM}}}{\sigma_{\text{SM}}^2} + \sum_{ij} \frac{C_i^{(6)} C_j^{(6)}}{\Lambda^4} \frac{\left(a_i^{(6)}\right)^2 \Delta \sigma_{\text{SM}} - a_i^{(6)} \Delta a_i^{(6)} \Delta \sigma_{\text{SM}} - b_{ij}^{(6)} \sigma_{\text{SM}} \Delta \sigma_{\text{SM}} + \Delta b_{ij}^{(6)} \sigma_{\text{SM}}^2}{\sigma_{\text{SM}}^3}$$

- $\sigma \equiv \sigma_F + \sigma_B$, $\Delta\sigma \equiv \sigma_F - \sigma_B$
- a_i, b_{ij} terms: SMEFT corrections
 - a_i : coefficients of terms linear in $C_i^{(6)}$
 - b_{ij} : coefficients of terms quadratic in $C_i^{(6)}$
- AFB expanded up to $\mathcal{O}(1/\Lambda^4)$, including dim-6 linear and quadratic contributions

No.	Exp.	\sqrt{s}	Obs.	Lumi. [fb^{-1}]	m_{ll}^{low} [GeV]
I	ATLAS ¹	8 TeV	$d\sigma/dm$	20.3	116 – 1000
II	CMS ²	13 TeV	$d\sigma/dm$	137 (ee) 140 ($\mu\mu$)	200 – 2210 (ee) 210 – 2290 ($\mu\mu$)
III	CMS ³	8 TeV	A_{FB}^*	19.7	120 – 500
IV	CMS ⁴	13 TeV	A_{FB}	138	170 – 1000

- 2 $d\sigma/dm$ data sets: (I & II)
- 2 AFB data sets: (III & IV)
- 2 data sets @8 TeV, $\sim 20 \text{ fb}^{-1}$ (I & III)
- 2 data sets @13 TeV, $\sim 140 \text{ fb}^{-1}$ (II & IV)
- include only high m_{ll} bins
- Experimental statistics & systematic uncertainties included
- no correlation across data sets

¹ Aad et al. 2016.

² Sirunyan et al. 2021.

³ Khachatryan et al. 2016.

⁴ Tumasyan et al. 2022.

No.	Exp.	\sqrt{s}	Obs.	Lumi. [fb^{-1}]	m_{ll}^{low} [GeV]
I	ATLAS	8 TeV	$d\sigma/dm$	20.3	116 – 1000
II	CMS	13 TeV	$d\sigma/dm$	137 (ee) 140 ($\mu\mu$)	200 – 2210 (ee) 210 – 2290 ($\mu\mu$)
III	CMS	8 TeV	A_{FB}^*	19.7	120 – 500
IV	CMS	13 TeV	A_{FB}	138	170 – 1000

- SM: **NLO QCD** + **NLL Sudakov**
 - **NNLO QCD** $\sim 2\%$ for most bins
 - **EW**: reach 10% for some high m_{ll} bins
- SMEFT: **LO in QCD**
 - NLO QCD corrections to SMEFT have no impact on the angular structure, thus won't change the flat directions
- PDF set: NNPDF 3.1 NNLO
- PDF uncertainties (SM): 100 replicas
- Scale uncertainties (SM): Envelope btw. 7 scales

$$\frac{1}{2} \leq \mu_{R,F}/\mu_0 \leq 2, \quad \frac{1}{2} \leq \mu_R/\mu_F \leq 2.$$

- ▶ First include only linear terms, where flat directions manifest
- ▶ Enabling 2 or 3 operators at a time
- ▶ Study 2-d bounds:
 - 2 cases that have flat directions
 - 2 cases that don't have flat direction, but still highly correlated

	A_1	A_2
u	$C_{eu}, C_{lq}^{(1)}, C_{lq}^{(3)}$	C_{lu}, C_{qe}
d	$C_{ed}, C_{lq}^{(1)}, C_{lq}^{(3)}$	C_{ld}, C_{qe}

Dependence of $A_{1,2}$ on $C^{(6)}$

- ▶ Show 68% CL bounds with:
 - one $d\sigma/dm$ data set only
 - one AFB data set only
 - combining all 4 $d\sigma/dm$ and AFB data sets ("combined" fit)

- In high energy limit, solve $\begin{cases} \sigma^u = 0 \\ \sigma^d = 0 \end{cases}$

	A_1	A_2
u	$C_{eu}, C_{lq}^{(1)}, C_{lq}^{(3)}$	C_{lu}, C_{qe}
d	$C_{ed}, C_{lq}^{(1)}, C_{lq}^{(3)}$	C_{ld}, C_{qe}

- Condition for both partonic channels to vanish after integration over c_θ^*

$$C_{ed}^{(1)} \equiv C_{ed} = C_{eu} \frac{Q_u e^2 - g_Z^2 g_L^u g_R^e}{Q_u e^2 - g_Z^2 g_R^e g_R^u} \frac{Q_d e^2 - g_Z^2 g_R^e g_R^d}{Q_d e^2 - g_Z^2 g_L^d g_R^e}$$

where the SM fermion couplings are: [Denner 1993](#)

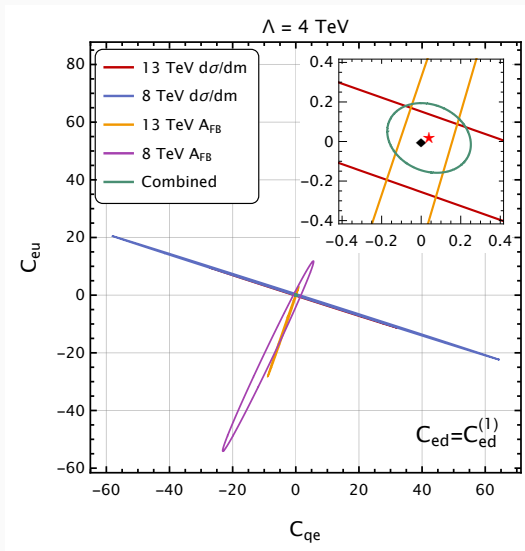
$$g_L^f = I_3^f - Q_f s_W^2, \quad g_R^f = -Q_f s_W^2.$$

- Flat direction in C_{qe} - C_{eu} plane when C_{ed} is fixed as $C_{ed}^{(1)}$
- C_{qe} & C_{eu} are in different A terms

➡ AFB can cancel out flat directions in $d\sigma/dm$

CASE I enabling C_{eu} , C_{ed} and C_{qe}

- $C_{ed} = C_{ed}^{(1)}$
 - both $d\sigma/dm$ and AFB exhibit flat directions
 - ellipses nearly orthogonal to each other
⇒ no flat direction in the combined fit
 - the bound is improved in the combined fit
- ◆ SM value (0, 0)
- ★ best fit



CASE II enabling C_{eu} , C_{ed} and $C_{lq}^{(1)}$

- In high energy limit, solve $\begin{cases} \sigma^u = 0 \\ \sigma^d = 0 \end{cases}$

	A_1	A_2
u	$C_{eu}, C_{lq}^{(1)}, C_{lq}^{(3)}$	C_{lu}, C_{qe}
d	$C_{ed}, C_{lq}^{(1)}, C_{lq}^{(3)}$	C_{ld}, C_{qe}

- Condition for both partonic channels to vanish after integration over c_θ^*

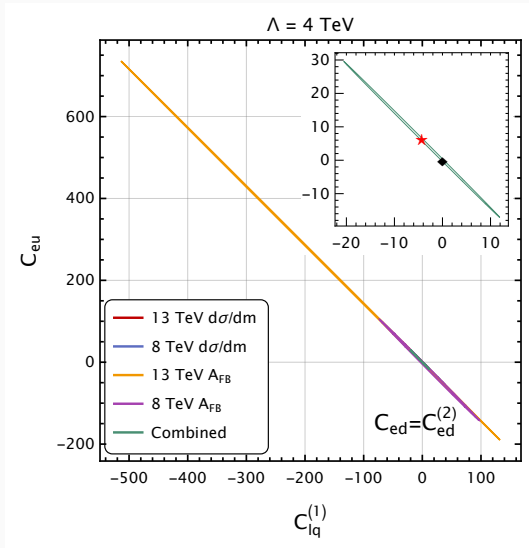
$$C_{ed}^{(2)} \equiv C_{ed} = C_{eu} \frac{Q_u e^2 - g_Z^2 g_R^u g_R^e}{Q_u e^2 - g_Z^2 g_L^e g_L^u} \frac{Q_d e^2 - g_Z^2 g_L^e g_L^d}{Q_d e^2 - g_Z^2 g_R^d g_R^e}$$

- Flat direction in $C_{lq}^{(1)} - C_{eu}$ plane when C_{ed} is fixed as $C_{ed}^{(2)}$
- $C_{lq}^{(1)}$ & C_{eu} are both in A_1

➡ AFB can not cancel out flat directions in $d\sigma/dm$

CASE II enabling C_{eu} , C_{ed} and $C_{lq}^{(1)}$

- $C_{ed} = C_{ed}^{(2)}$
 - both $d\sigma/dm$ and AFB exhibit flat directions
 - ellipses pointing at the same direction
 \Rightarrow flat direction still in the combined fit
 - AFB does not remove the degeneracy, nor improve the bound
- ◆ SM value (0, 0)
- ★ best fit



- In high energy limit, solve $\begin{cases} \sigma^u = 0 \\ \sigma^d = 0 \end{cases}$
- up-quark channel:

$$C_{lq}^{(1)} = -C_{qe} \frac{Q_u e^2 - g_Z^2 g_L^u g_R^e}{Q_u e^2 - g_Z^2 g_L^e g_L^u}$$

- down-quark channel:

$$C_{lq}^{(1)} = -C_{qe} \frac{Q_d e^2 - g_Z^2 g_L^d g_R^e}{Q_u e^2 - g_Z^2 g_L^e g_L^d}$$

- no common solution \Rightarrow no flat direction

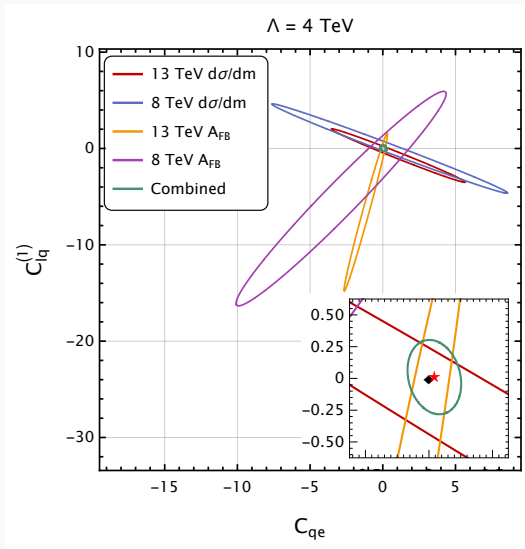
CASE III enabling C_{qe} and $C_{lq}^{(1)}$

	A_1	A_2
u	$C_{lq}^{(1)}$	C_{qe}
d	$C_{lq}^{(1)}$	C_{qe}

- C_{qe} & $C_{lq}^{(1)}$ are highly correlated
- C_{qe} & $C_{lq}^{(1)}$ are in different A terms
 \Rightarrow ellipses with $d\sigma/dm$ & AFB pointing in opposite directions
- bound improved in the combined fit

◆ SM value (0, 0)

★ best fit



CASE IV enabling $C_{lq}^{(1)}$ and $C_{lq}^{(3)}$

- In high energy limit, solve $\begin{cases} \sigma^u = 0 \\ \sigma^d = 0 \end{cases}$
- up-quark channel depends on the combination $C_{lq}^{(1)} + C_{lq}^{(3)}$
- down-quark channel depends on the combination $C_{lq}^{(1)} - C_{lq}^{(3)}$
- no common solution \Rightarrow no flat direction

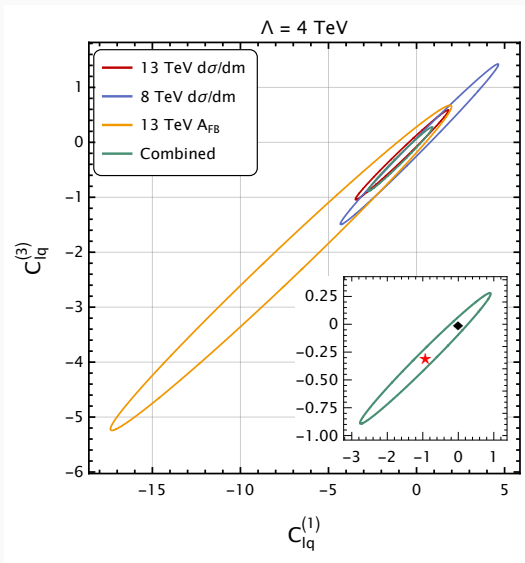
CASE IV enabling $C_{lq}^{(1)}$ and $C_{lq}^{(3)}$

	A_1	A_2
u	$C_{lq}^{(1)}, C_{lq}^{(3)}$	
d	$C_{lq}^{(1)}, C_{lq}^{(3)}$	

- $C_{lq}^{(1)}$ & $C_{lq}^{(3)}$ are highly correlated
- $C_{lq}^{(1)}$ & $C_{lq}^{(3)}$ are both in A_1
 \Rightarrow ellipses with $d\sigma/dm$ & AFB pointing in the same direction
- bound not improved in the combined fit

◆ SM value (0, 0)

★ best fit

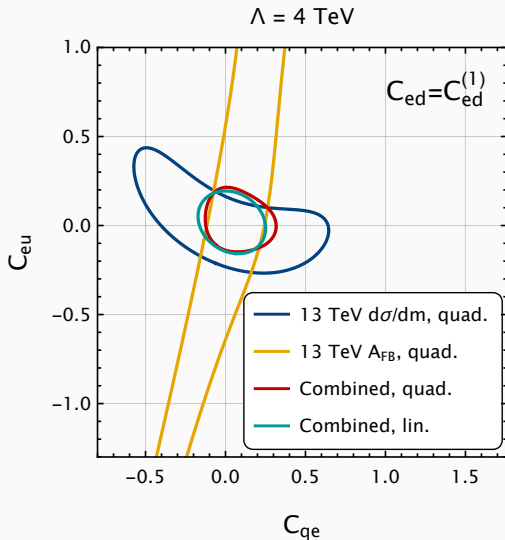


LO SMEFT contributions to partonic cross section in high energy limit

$$\frac{d\sigma^x}{dm_{ll}^2 dY dc_\theta^*} \sim \frac{1}{\Lambda^2} \frac{A_1^x \hat{u}^2 + A_2^x \hat{t}^2}{\hat{s}^2} + \frac{1}{\Lambda^4} (B_1^x \hat{u}^2 + B_2^x \hat{t}^2)$$

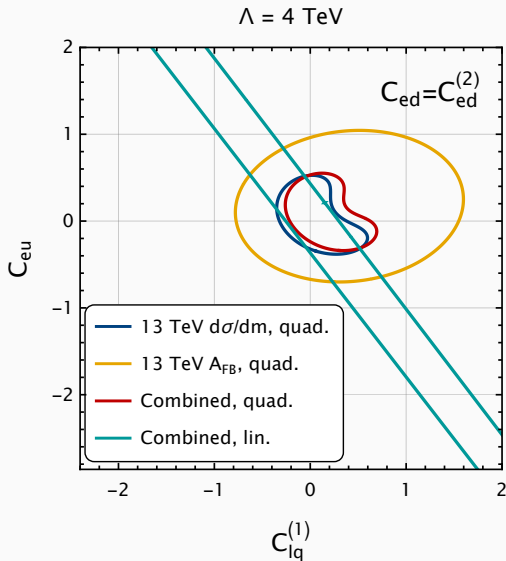
- $B_1^u \propto C_{eu}^2 + \left(C_{lq}^{(1)} - C_{lq}^{(3)}\right)^2$
- $B_1^d \propto C_{ed}^2 + \left(C_{lq}^{(1)} + C_{lq}^{(3)}\right)^2$
- $B_2^u \propto C_{lu}^2 + C_{qe}^2$
- $B_2^d \propto C_{ld}^2 + C_{qe}^2$
- Adding quadratic terms breaks flat directions appearing in linear terms

- $C_{ed} = C_{ed}^{(1)}$
- Single data set: **Quadratic contributions break degeneracies**
- Combined fit:
 - **Linear: AFB cancels degeneracies in $d\sigma/dm$**
 - Adding quadratic contributions to combined fit: **no improvement**

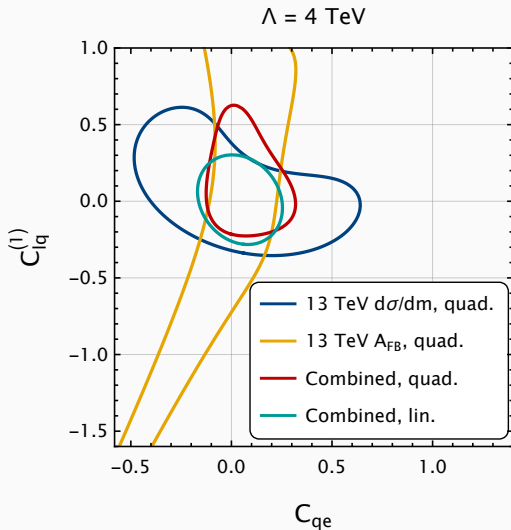


CASE II W/ QUADRATIC TERMS enabling C_{eu} , C_{ed} and $C_{lq}^{(1)}$

- $C_{ed} = C_{ed}^{(2)}$
- Single data set: **Quadratic contributions break degeneracies**
- Combined fit:
 - Linear: **AFB can not cancel degeneracies in $d\sigma/dm$**
 - Quadratic contributions **improve the combined fit significantly**

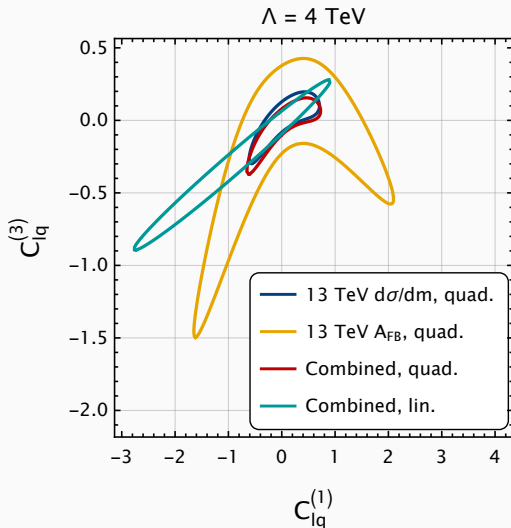


- strong correlation but no flat directions
- Single data set: **Quadratic contributions reduce correlations**
- Combined fit:
 - **Linear: Combining AFB & $d\sigma/dm$ reduces correlation**
 - Little differences btw. **linear** and **quadratic combined fits**

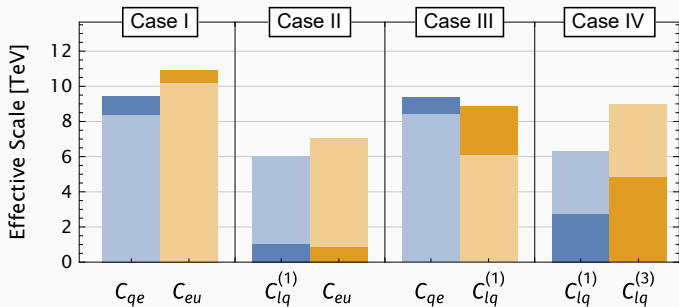


CASE IV W/ QUADRATIC TERMS enabling $C_{lq}^{(1)}$ and $C_{lq}^{(3)}$

- strong correlation but no flat directions
- Single data set: **Quadratic contributions reduce correlations**
- Combined fit:
 - **Linear:** Narrow ellipse \Rightarrow Supplementing $d\sigma/dm$ w/ AFB is unable to reduce such correlation
 - **Quadratic contributions improve the combined fit significantly**



EFFECTIVE SCALE



- Effective scales M from 68% CL bounds (choosing $g = 1$, $\Lambda = 4$ TeV)

$$\frac{C}{\Lambda^2} \sim \frac{g^2}{M^2}$$

- Include only the combined fit
 - ▶ darker bars: only linear terms
 - ▶ lighter bars: quadratic terms included
- improvement from quadratic terms in case II & IV (where AFB didn't help), but not I & III

- Combining measurements of $d\sigma/dm$ and AFB in neutral-current Drell-Yan
- Fits to the four-fermion sector of the SMEFT at dimension-6
- In some cases (case I & III):
 - AFB can break degeneracies in $d\sigma/dm$
 - Even when there's no flat direction, if two operators are highly correlated, AFB can drastically improve bounds
 - Quadratic corrections are negligible in the combined fit
- In other cases (case II & IV):
 - AFB can not fix flat directions in $d\sigma/dm$
 - When there's no flat direction but two operators are highly correlated, AFB provides no improvement on bounds
 - Quadratic corrections are important in the combined fit

Thanks for your attention!

Backup

- A_{FB}^* : quark direction approximated w/ dilepton momentum

$$\cos \theta_R = \frac{|Q^z|}{Q^z} \cos \theta^*.$$

Asymmetry diluted when quark direction not aligned with dilepton direction (e.g. small $|y|$ region)

- A_{FB} (the "true" AFB): using Monte-Carlo as template, identify quark direction at parton level [Tumasyan et al. 2022](#); [Accomando et al. 2016](#)
 - Gluon initiated processes: In our calculations, we assign quark direction that's consistent with the cancellation of collinear singularities
i.e. $g\bar{q}$: quark direction set to gluon direction
 - Huge scale uncertainties, higher order effects

- No correlation between the data sets
- Data set I: experimental uncertainties provided by ATLAS, including full statistical and systematic errors
- Rest of the data sets: no correlated systematic error provided
 - Data set II: assume no correlation between different bins & channels
 - Data set III: assume no correlation between different bins, it's tested that the correlations have little effect
 - Data set IV: assume no correlation between different bins, same as data set III
- Theoretical uncertainties:
 - correlated PDF errors across bins and data sets
 - uncorrelated scale uncertainties
 - NNLO QCD corrections less than 2% for most bins
 - electroweak corrections as much as 10% for high $m_{\ell\ell}$ bins
 - Scale choice: $\mu_0 = m_{\ell\ell}$ for data set I, II, III
 - Data set IV: Use $\mu_0 = H_T$ ⁵ as the central value. Calculate both $\mu_0 = m_{\ell\ell}$ & $\mu_0 = H_T$ along with their 6 scale variations, then take the envelope.

⁵ H_T is the sum of transverse masses of all final state particles

EVENT NUMBERS IN DATA SET II

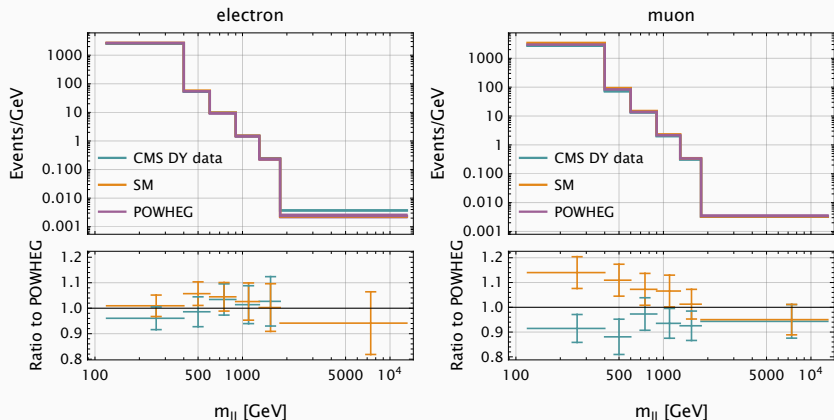


Figure: Event yields in the electron (left) and muon (right) channels for the 13 TeV data set II. The green lines show the observed total event yields minus all non-Drell-Yan backgrounds. The orange lines show our SM predictions with electroweak Sudakov corrections. The purple line shows the POWHEG estimate for the Drell-Yan background. The lower inset shows the ratio to the Drell-Yan background estimations in Ref. Sirunyan et al. 2021. The error bars represent uncertainties from the POWHEG estimates.

SCALE CHOICE W/ DATA SET IV

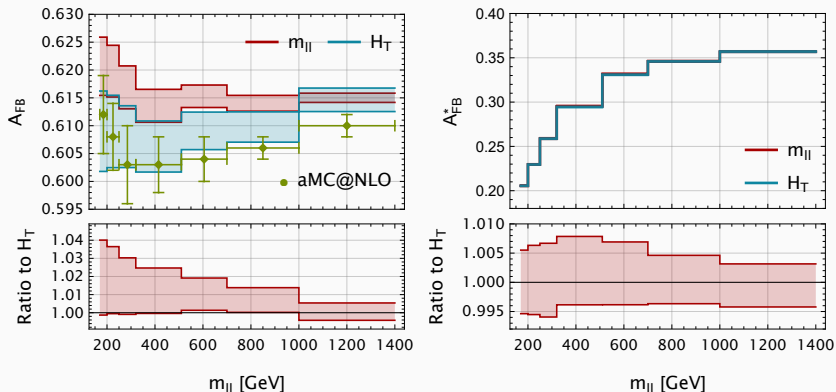


Figure: Left panel: The “true” forward-backward asymmetry A_{FB} for data set IV with dynamic scale $\mu_0 = m_{II}$ (red) and $\mu_0 = H_T$ (blue). The bands represent the range of scale variation ($1/2 \leq \mu_{R,F}/\mu_0 \leq 2$, $1/2 \leq \mu_R/\mu_F \leq 2$) for both scale choices. The aMC@NLO simulation in Ref. Tumasyan et al. 2022 is shown by the green points. Right panel: the same comparison for A_{FB}^* .

CASE I: CONDITION FOR X-SEC TO VANISH

- Receive contributions from $A_1^u(C_{eu}), A_1^d(C_{ed}), A_2^{u/d}(C_{qe})$
- Contributions from all 3 operators won't vanish simultaneously
 \Rightarrow pick one slice in $C_{qe} - C_{eu}$ plane where flat direction is present
- Conditions for the **cross section to vanish** after integration over c_{θ}^* for each channel

$$u : C_{qe} = -C_{eu} \frac{Q_u e^2 - g_Z^2 g_L^u g_R^e}{Q_u e^2 - g_Z^2 g_R^e g_R^u},$$

$$d : C_{qe} = -C_{ed} \frac{Q_d e^2 - g_Z^2 g_L^d g_R^e}{Q_d e^2 - g_Z^2 g_R^e g_R^d},$$

the SM left-handed and right-handed fermion couplings: [Denner 1993](#)

$$g_L^f = I_3^f - Q_f s_W^2, \quad g_R^f = -Q_f s_W^2.$$

- These conditions are simultaneously satisfied when

$$C_{ed}^{(1)} \equiv C_{ed} = C_{eu} \frac{Q_u e^2 - g_Z^2 g_L^u g_R^e}{Q_u e^2 - g_Z^2 g_R^e g_R^u} \frac{Q_d e^2 - g_Z^2 g_R^e g_R^d}{Q_d e^2 - g_Z^2 g_L^d g_R^e}$$

DIM-8 EFFECTS

- Relevant operators: $\psi^4 D^2$

i.e.

$$\mathcal{O}_{q^2 e^2 D^2}^{(2)} = \left(\bar{e} \gamma^{(\mu} \overleftrightarrow{D}^{\nu)} e \right) \left(\bar{q} \gamma_{\mu} \overleftrightarrow{D}_{\nu)} q \right)$$

- Shaded area:
1-d bounds of single Wilson
coefficient

